

Lithium in population I subgiants^{*}

S. Randich¹, R. Gratton², R. Pallavicini³, L. Pasquini⁴, and E. Carretta²

¹ Osservatorio Astrofisico di Arcetri, Largo Fermi 5, I-50125 Firenze, Italy (randich@arcetri.astro.it)

² Osservatorio Astronomico di Padova, Vicolo dell' Osservatorio 5, I-35122 Padova, Italy

³ Osservatorio Astronomico di Palermo, Piazza del Parlamento 1, I-90136 Palermo, Italy

⁴ European Southern Observatory, Karl-Schwarzschild-Strasse 2, D-85748 Garching, Germany

Received 27 January 1999 / Accepted 4 June 1999

Abstract. We present a lithium survey for a sample of 91 Pop. I stars. *JHKL* photometry was also obtained for 61 stars in the sample. Besides Li abundances, [Fe/H] values were derived. Thanks to Hipparcos parallaxes, we could infer absolute V magnitudes for our sample stars and were able to place them on the color–magnitude diagram, which allowed us to constrain their evolutionary status. Masses and ages were derived for most of the stars by comparison with evolutionary tracks. The sample was originally selected so to include class IV stars later than spectral-type F0, but, based on the location on the color–magnitude diagram, we found *a posteriori* that a fraction of the stars (about 20%) are either main sequence stars or evolved giants.

As it is the case for dwarfs and giants, a large spread in lithium abundance is present among the subgiants in our sample. As expected, the average lithium decreases as the stars evolve along the subgiant branch; however, there is not a one-to-one relationship between the position on the color–magnitude diagram and lithium abundance, and the observed dispersion is only partially explainable as due to a dispersion in mass, metallicity, and age. In particular, a dispersion in lithium is seen among slightly evolved subgiants with masses close to solar but in the same evolutionary stage as the G2 IV star β Hyi. The comparison of the β Hyi-like sample with a sample of non evolved solar-like stars indeed suggests that β Hyi has most likely evolved from a main sequence Li-rich star, rather than from a Li-poor star (like the Sun) that has dredged-up previously stored lithium.

Our sample includes several stars that have completed the first-dredge up lithium dilution, but that have not yet evolved to the evolutionary point where extra-mixing in the giant phase is thought to occur. A large number of them have Li abundances considerably below the theoretical predictions of first dredge-up dilution. We confirm that this is due to the fact that the progenitors of these stars are most likely stars that have depleted lithium while on the main sequence; the fraction of post-dredge up Li rich/poor stars, in fact, is consistent with the observed distribution of Li abundances among stars that have just left the main sequence.

The signature of the second mixing (or RGB extra-mixing) episode is evident in the $\log n(\text{Li})$ vs. $B-V$ and $\log n(\text{Li})$ vs. M_{bol} distributions of the stars in the sample; it seems however that the extra-mixing occurs at luminosities lower than predicted by the models of Charbonnel (1994).

Finally, a few evolved giants are found that should have passed the second mixing episode, but that do not show signs of it. At least half of them are spectroscopic binaries.

Key words: stars: abundances – stars: fundamental parameters – stars: late-type

1. Introduction

The evolution of surface lithium abundance is far from being understood and the stellar lithium content is not easily predictable as a function of age, evolutionary status, mass, and metallicity. It is now well established that, with the exception of very low mass stars, convection is neither the only one nor the main mixing mechanism. Non standard mixing-processes acting during residence on the main sequence (MS) are indeed required in order to explain several observed features, such as, for example, the fact that solar-type stars destroy lithium while on the MS, as evidenced by the difference between the 120 Myr Pleiades and the 700 Myr old Hyades (but see Swenson et al. 1994a,b for an alternative interpretation), or the significant lithium depletion observed in a fraction of F-type stars with very thin convective zones when they leave the MS (Balachandran 1990).

The Sun, whose low lithium abundance cannot be explained by standard models including convection only, is probably the best known example of the need for an additional (or extra) mixing mechanism acting on the MS (e.g., Chaboyer et al. 1995; Pinsonneault 1997 and references therein). Both in the field and in the open cluster M67 (which has solar age and metallicity) solar-type stars are observed with a lithium content as low as or even lower than in the Sun; at the same time, however, a high percentage of the stars have a factor of ten higher lithium or more (Spite et al. 1987; García López et al. 1988; Pasquini et al. 1994; Pasquini et al. 1997). The G2 IV star β Hyi is a well known example of an old, but lithium rich star. It is slightly more massive than the Sun, but it is older and in a more advanced

Send offprint requests to: S. Randich

^{*} Based on observations carried out at the European Southern Observatory, La Silla, Chile

evolutionary stage (see Dravins et al. 1993, 1998); its lithium abundance is a factor ~ 30 higher than in the Sun. Dravins et al. (1993) suggested that Li could have diffused downward during MS lifetime, and temporarily stored below the convective zone. As the star evolves off the MS, Li could be dredged-up to the surface, thus leading to a short-lived enhancement of surface Li abundance before appreciable dilution occurs. According to this scenario, the high lithium content of β Hyi is linked to its evolutionary status and, in principle, the Sun should also pass through a short phase of lithium enrichment. On the other hand, the alternative hypothesis can be made that, as it is the case for the lithium-rich old solar-type stars in M67 or in the field, β Hyi left the MS with a high lithium content which, therefore, would just be the result of a reduced mixing (with respect to the Sun) during MS lifetime.

Observations of giant stars also challenge our understanding of lithium evolution. In principle, the lithium content of giants after the first dredge-up has occurred should be simply the product of the lithium content at the end of the MS times the dilution factor due to the deepening of the convective envelope and to the mixing with lithium depleted material. The first calculations of lithium dilution during post-main sequence phases were carried out by Iben (1965; 1967ab) who predicted a factor of about 28 and 60 Li dilution at the end of the first dredge-up for $1-1.5 M_{\odot}$ and $3-5 M_{\odot}$, respectively; therefore, lithium abundances of the order of $\log n(\text{Li})=1.85$ and 1.5 should be observed for stars which left the MS with their original lithium content ($\log n(\text{Li})\sim 3.3$). Evolved giant stars in several clusters with different ages and turn-off masses (Gilroy 1989) and in the field (Brown et al. 1989) show lithium abundances that are not in agreement with these theoretical predictions since they are, on average, lower than the predicted maximum values. At least two different, but complementary explanations for this have been proposed. First, stars that, for whatever reason, show apparent signs of lithium depletion at the end of their MS lifetime, will have $n(\text{Li})$ below the predictions once they evolve to the giant branch. Second, an extra-mixing mechanism acting during some phases of the post-main sequence evolution is also likely to be at work. The need for a mixing mechanism which adds to the first dredge-up is also evidenced by measurements of the $^{12}\text{C}/^{13}\text{C}$ and $^{12}\text{C}/^{14}\text{N}$ ratios in evolved stars in open and globular clusters: observed post dredge-up values of those ratios are in agreement with the theoretical predictions, but, at a later stage in the evolution along the giant branch, they become substantially lower (e.g., Charbonnel 1995 and references therein). Observations of CNO elements suggest that the extra-mixing process acts only in stars with masses $< 2 M_{\odot}$ and that it becomes efficient when the stars reach the so-called luminosity bump or RGB bump; this corresponds to the evolutionary point where the hydrogen burning shell crosses the chemical discontinuity left by the convective envelope at its maximum extent; for stars that have not reached this point the mean molecular weight gradient constitutes a barrier to any mixing mechanism (e.g., Charbonnel 1994; Charbonnel 1995; Charbonnel et al. 1998).

We present here a lithium survey for a sample of nearly 100 Pop. I stars, a large fraction of which are in the subgiant evolutionary phase. Whereas the distribution of lithium among dwarf and giant field stars is observationally well constrained (although not so well understood), additional information for the intermediate evolutionary stages is certainly needed. Our primary goal is to follow the evolution of lithium from the latest phases on the MS to the first ascent of the giant branch; more specifically, we intend to use a large sample of stars to investigate the dependence of lithium on evolutionary status and mass, disentangling the effect of the other stellar parameters (e.g., metallicity). Our sample contains stars just evolved-off the main sequence which are in an evolutionary stage similar to that of β Hyi, and should allow us to further investigate the diffusion mechanism proposed by Dravins et al. (1993). In addition, several stars in our sample are crossing the Hertzsprung gap or are approaching the first ascent giant phase; these objects will allow us to put further constraints both on the first dredge-up dilution and on the signatures of the extra-mixing.

Observations of subgiant stars have sparsely been carried out within various lithium surveys of field stars (e.g., Pallavicini 1987 and reference therein). However, to our knowledge, only four lithium surveys specifically focussed on subgiants were carried out in the last decade. Balachandran (1990) derived lithium abundances for a sample of 200 F stars slightly evolved off the MS. Her primary goal was to investigate the processes of lithium depletion during MS lifetime for these rather warm stars. Her sample is complementary to ours, since it includes on average more massive and less evolved stars; we will use this sample to complement our one. Pilachowski et al. (1993) determined lithium for 79 metal poor ($[\text{Fe}/\text{H}] < -1.4$) subgiants with the purpose of studying lithium dilution; their results are consistent with the indications that come from CNO elements. They found a qualitative agreement with first dredge-up predictions for stars warmer than 4900 K, but their data suggested that additional Li destruction and extra-mixing should occur for cooler stars. Similar results were obtained by Carretta et al. (1998) for a sample of metal poor stars ($[\text{Fe}/\text{H}] < -1$). We consider these samples also as complementary to ours, both because of the different metallicity and because of the restricted range of masses of halo subgiants in comparison with Pop. I subgiants. Very recently a study of lithium in subgiant stars was carried out by De Medeiros et al. (1997) who, however, used lithium abundances from the literature and investigated the relationship between lithium depletion and rotation, rather than following lithium evolution itself.

2. The sample

Our sample contains 91 stars later than spectral-type F0 with declination $\delta \leq +10$ selected from the Bright Star Catalogue (Hoffleit & Jascheck 1982). The sample selection was carried out on the basis of the published spectral types and, therefore, our sample includes also stars with uncertain luminosity class (IV-V or IV-III) which eventually turned out to be dwarfs or evolved giants from their position on the color-magnitude (C-

Table 1. The sample stars

HD #	Sp.	M_V	$B-V$	$b-y$	$v \sin i$ (km s^{-1})	note
142	G1 IV	3.66	0.519	0.331 ⁽¹⁾	–	
469	G4 IV	0.55	0.738	0.459 ⁽¹⁾	–	sb
645	K0 IV	1.77	1.000	0.613 ⁽³⁾	1.3	
3303	K0 IV	1.59	1.001	–	1.0	
6269	G5 IV	1.03	0.932	0.576 ⁽²⁾	4.6	
8779	K0 IV	-0.22	1.241	0.759 ⁽²⁾	1.0	
9562	G2 IV	3.39	0.639	0.398 ⁽¹⁾	4.1	
10142	K0 IV	0.96	1.045	0.644 ⁽¹⁾	2.3	
11332	K1 IV	0.25	0.998	–	2.2	
12583	G3 IV	0.85	0.966	0.595 ⁽¹⁾	–	
13421	G0 IV	2.50	0.569	0.358 ⁽⁵⁾	9.9	
16589	G0 IV	2.84	0.521	0.338 ⁽⁵⁾	34.2	sb
18262	F7 IV	2.73	0.478	0.304 ⁽⁵⁾	9.9	
18907	G5 IV	3.47	0.794	0.498 ⁽¹⁾	1.3	
19826	K0 IV	1.74	0.912	0.576 ⁽¹⁾	2.5	sb
26913	G5 IV	5.34	0.680	0.420 ⁽⁵⁾	4.7	
26923	G0 IV	4.69	0.570	0.368 ⁽⁵⁾	3.3	
27442	K2 IV	3.14	1.078	0.651 ⁽¹⁾	1.2	
29613	K1 IV	1.54	1.054	0.645 ⁽¹⁾	1.0	
30608	K1 IV	0.36	1.071	–	–	
34642	K0 IV	2.17	0.987	0.601 ⁽⁴⁾	1.0	
36553	G3 IV	2.26	0.615	0.390 ⁽¹⁾	–	
37501	G5 IV	1.18	0.845	–	–	
39937	F7 IV	0.41	0.656	0.410 ⁽¹⁾	8.6	sb
40105	G8 IV	3.82	0.891	0.557 ⁽¹⁾	–	
41700	G0 IV-V	4.22	0.517	0.346 ⁽¹⁾	16.2	
50806	G5 IV	3.99	0.708	0.437 ⁽¹⁾	–	
51825	F8 IV-V	3.05	0.465	0.305 ⁽⁵⁾	28.3	
62644	G6 IV	3.13	0.765	0.471 ⁽¹⁾	–	
66011	G0 IV	2.34	0.570	0.360 ⁽⁵⁾	13.6	
72954	G5 IV-V	2.42	0.752	0.472 ⁽¹⁾	3.8	sb
80170	K5 III-IV	0.12	1.166	–	1.5	
82074	G6 IV	2.57	0.838	0.506 ⁽¹⁾	2.1	
82734	K0 IV	-0.03	1.023	0.624 ⁽¹⁾	3.8	
85655	K2 IV	-1.01	1.354	–	1.4	sb
90170	G8 IV	1.98	0.884	–	1.4	
92588	K1 IV	3.57	0.880	0.531 ⁽²⁾	1.1	
94386	K3 IV	1.91	1.176	–	1.0	
99491	K0 IV	5.25	0.778	0.484 ⁽¹⁾	2.6	
100219	F7 IV	3.26	0.537	0.339 ⁽⁵⁾	5.2	
104055	K2 IV	-0.13	1.257	–	2.0	
104307	K0 IV	0.22	1.220	–	1.0	sb
107773	G8-K0 IV	2.83	0.887	0.557 ⁽¹⁾	1.3	
114837	F7 IV	3.62	0.489	0.321 ⁽⁵⁾	9.7	sb
120237	G3 IV-V	4.30	0.561	0.357 ⁽¹⁾	–	
121056	K1 IV-V	2.13	1.009	0.627 ⁽¹⁾	1.4	
121384	G6 IV-V	3.09	0.780	0.481 ⁽⁵⁾	1.4	sb
125184	G2 IV	3.89	0.723	0.454 ⁽¹⁾	1.1	
126400	G7 IV	2.05	0.941	–	–	
126868	G2 IV	1.72	0.693	0.437 ⁽¹⁾	14.3	
140301	K0 IV	0.80	1.124	–	1.0	
144585	G4 IV-V	4.02	0.660	0.410 ⁽²⁾	2.7	sb
145148	K0 IV	3.51	0.988	0.605 ⁽¹⁾	1.0	
147723	G0 IV	–	0.590	0.377 ⁽⁵⁾	–	

Table 1. (continued)

HD #	Sp.	M_V	$B-V$	$b-y$	$v \sin i$ (km s^{-1})	note
152781	K0 IV	3.30	0.952	–	1.0	
154556	K1 IV	1.99	1.062	–	1.0	
155974	G0 IV-V	3.55	0.478	0.321 ⁽⁴⁾	7.2	
156846	G3 IV	3.05	0.578	0.365 ⁽²⁾	4.9	
157347	G5 IV	4.83	0.680	0.426 ⁽¹⁾	1.1	
160691	G3 IV-V	4.20	0.694	0.432 ⁽¹⁾	1.7	
165438	K1 IV	3.02	0.968	0.594 ⁽³⁾	1.0	
165978	K0 IV	1.15	1.025	0.635 ⁽¹⁾	1.8	
166599	K0 III-IV	0.79	0.944	–	4.3	
169233	K0 III-IV	-0.93	1.138	–	1.0	
170525	G5 IV	2.89	0.688	0.430 ⁽⁵⁾	2.7	
172223	K2 III-IV	0.78	1.220	–	2.6	
173902	K1 IV	1.88	1.085	–	1.0	
177389	G8-K0 III-IV	2.48	0.901	–	1.0	
177565	G5 IV	4.98	0.705	0.437 ⁽¹⁾	3.2	
188512	G8 IV	3.03	0.855	0.521 ⁽⁵⁾	1.2	
191067	K1 IV	2.57	1.023	0.625 ⁽¹⁾	1.0	sb
194433	K2 IV-V	3.25	0.961	0.596 ⁽¹⁾	2.1	
195564	G2.5 IV	3.74	0.689	0.431 ⁽¹⁾	1.8	
196755	G5 IV	2.68	0.702	0.432 ⁽¹⁾	3.5	
199223	G6 III-IV	0.82	0.824	0.525 ⁽²⁾	1.0	
200011	G3 IV	2.09	0.663	0.424 ⁽¹⁾	2.5	
200073	K0 IV	1.84	1.106	0.680 ⁽⁴⁾	2.7	
202773	G8 IV	0.94	0.966	0.615 ⁽¹⁾	1.6	
210434	K0 III-IV	1.30	0.981	0.596 ⁽³⁾	3.3	
211391	G8 III-IV	0.33	0.979	0.594 ⁽¹⁾	1.6	
212330	G3 IV	3.75	0.665	0.424 ⁽¹⁾	1.5	sb
214599	K0 IV	0.53	1.006	0.607 ⁽²⁾	1.0	
216385	F7 IV	3.02	0.487	0.316 ⁽¹⁾	5.7	
216437	G2-3 IV	3.92	0.660	0.422 ⁽¹⁾	3.7	
216718	K0 III-IV	0.95	0.881	0.545 ⁽³⁾	2.6	
217107	G8 IV	4.70	0.744	0.455 ⁽¹⁾	1.7	
217703	K0 III-IV	1.54	0.946	0.581 ⁽¹⁾	2.0	
219834	G5 IV	3.62	0.787	0.476 ⁽¹⁾	2.9	sb
223524	K0 IV	1.06	1.133	0.703 ⁽³⁾	1.0	
224022	F8 IV	3.80	0.572	0.364 ⁽⁵⁾	5.4	
224750	G3 IV	1.97	0.763	–	6.1	

Sources for $b-y$ colors: (1) Olsen (1993); (2) Olsen (1983); (3) Anthony-Twarog et al. (1991) (4) Schuster & Nissen (1988); (5) Hauck & Mermilliod (1980).

M) diagram based on Hipparcos parallaxes. More specifically, 70 of the stars are class IV stars, whereas the remaining 21 are classified as IV-V or IV-III. The sample stars are listed in Table 1. HD numbers are given in Column 1, while basic information are listed in Columns 2–5; $v \sin i$ values and notes on binarity are given in the last two columns of the table. The information on spectral types was taken from the Bright Star Catalogue itself: in most cases, the spectral classification is the same as given in the Simbad database, although for a few stars differences in the luminosity class are present. $B-V$ colors, V magnitudes and parallaxes and, therefore, absolute magnitudes M_V were retrieved from the Hipparcos catalogue; $b-y$ colors

were taken from various sources in the literature as indicated in the table's notes. Rotational velocities and information on binarity, obtained using Coravel, were kindly provided by Dr. De Medeiros.

As we will show in the following sections, the sample includes stars in a range of masses, metallicities, evolutionary stages, and, obviously ages. It is, however, a magnitude limited sample (but we caution that it is not complete), and therefore it should be unbiased with respect to kinematics, chemical composition, activity, and rotation. This on the one hand allows us to investigate the issue of lithium abundance for an unbiased sample and, on the other hand, to investigate the dependence of lithium itself on at least some of the above parameters.

3. Observations

The spectroscopic observations were carried out at ESO La Silla in two different observing runs, in May and October 1992. The 1.4m Coudé Auxiliary Telescope (CAT) with the Coudé Echelle Spectrograph (CES; Kaper & Pasquini 1996) in combination with a Short Camera and ESO CCD #9 was used. With such a configuration we achieved a resolving power $R = 60,000$ and a spectral range of 53 \AA centered at $\lambda = 6708 \text{ \AA}$. Typical S/N ratios for the sample stars are in the range $\sim 100\text{--}150$, with a very few stars having a slightly lower S/N. The data were reduced using MIDAS and following the usual steps: namely, bias subtraction, flat fielding, and wavelength calibration. The spectra can be made available by SR or LP under request.

Near IR (NIR) photometric observations in the J , H , K , L bands for about 70% of the stars in the sample were kindly carried out at La Silla by Dr. P. Bouchet and R. Vega on October 8–14 1992. The 1m telescope equipped with the ESO IR photometer and InSb detector (Bouchet 1989) was used. The photometry was obtained using the ESO standard stars system (Bouchet et al. 1991). Data reduction was carried out assuming the standard values of the atmospheric extinction coefficients at La Silla, namely: $E_J = 0.125$, $E_H = 0.080$, $E_K = 0.110$, and $E_L = 0.170 \text{ mag/airmass}$. Most of the stars were observed at low airmass and thus systematic errors due to atmospheric extinction are typically below 1%. The statistical errors are in the range 0.1–2%. Whereas part of the stars were observed only once, others had two or more observations. In those cases the weighted mean of the single measurements was adopted; for all the stars observed more than once no significant differences among the different measurements were found. J , H , K , L magnitudes are listed in Table 2.

4. Abundance analysis

4.1. Atmospheric parameters

The abundance analysis was carried out for most stars in the sample by means of equivalent widths, following an iterative procedure similar to that described in Clementini et al. (1999). A first order set of parameters was estimated as follows: Initial metal abundances were estimated from the *ubv* photometry and using the calibration by Schuster & Nissen (1989). For

stars with no *ubv* photometry available an initial $[\text{Fe}/\text{H}] = 0$ was assumed. Initial effective temperatures (T_{eff}) were derived using both the colors from our NIR photometry (specifically, $J\text{--}K$ and $V\text{--}K$) and $B\text{--}V$ and $b\text{--}y$ colors from the literature. The empirical calibration of Gratton et al. (1996) for population I stars and the abundance dependence given by Kurucz (1993) models were employed. Surface gravities $\log g$ were determined using the relation:

$$\log g = 0.4 (M_V + BC - 4.72) + \log M/M_{\odot} + 4 \log T_{\text{eff}} - 10.60$$

where BC are the bolometric corrections (from Kurucz, 1993) and masses were derived as explained in Sect. 4.3. A mass $M = 1.3M_{\odot}$ –the average for the stars for which we determined the mass– was assumed for the stars with unknown mass. Finally, microturbulence velocities were estimated using the relationship:

$$\xi = -0.322 \log g + 2.22 \text{ km s}^{-1} \quad (\text{Gratton et al. 1996}).$$

The equivalent widths were analyzed using the first order stellar parameters and $[\text{Fe}/\text{H}]$ values were determined (see next section). While $\log g$ and ξ were then kept fixed, T_{eff} were derived again based on the new $[\text{Fe}/\text{H}]$; the procedure was iterated until a consistent set of parameters was obtained. The final T_{eff} together with $\log g$ values are listed in the second and third columns in Table 3.

Errors in the atmospheric parameters are as follows: we estimated random errors in T_{eff} by comparing temperatures derived from different color indices, obtaining a mean quadratic error equal to $\pm 42 \text{ K}$. Systematic errors due to the adopted T_{eff} scale may be larger, but still $\leq 100 \text{ K}$, as discussed in detail in Gratton et al. (1996). Finally, a contribution to the errors in T_{eff} is given by neglecting the reddening (the internal error is of the order of $\pm 50 \text{ K}$). As to gravities and microturbulence, we estimate that the errors should be of the order of $\pm 0.25\text{--}0.3 \text{ dex}$ for $\log g$ and of the order of $\pm 0.3 \text{ km s}^{-1}$ for ξ .

4.2. Metallicities and lithium abundances

$[\text{Fe}/\text{H}]$ values have been determined using the Fe I lines included in the spectral range covered by our observations. The number of lines used for the analysis varies between four and eight (namely, $\lambda = 6699.142 \text{ \AA}$, 6703.572 \AA , 6704.485 \AA , 6710.322 \AA , 6713.745 \AA , 6725.358 \AA , and 6726.671 \AA , 6733.157 \AA), depending on the quality of the spectrum. The equivalent widths (EWs) of the above lines have been measured by means of a Gaussian fitting routine applied to the core of the lines; EWs can be made available by one of us (RG) under request. Kurucz (1995) model atmospheres and the same line parameters and solar abundances (in particular $\log \epsilon(\text{Fe})_{\odot} = 7.52$) used by Carretta & Gratton (1997) were adopted; g_f values had been derived by carrying out an analysis of the solar spectrum, using EWs measured on the spectrum of the solar flux (Kurucz et al. 1984). The *rms* of the $[\text{Fe}/\text{H}]$ obtained from the single lines is comprised between 0.020 and 0.165 dex (but is larger than 0.1

Table 2. Near-infrared photometry

HD	J	H	K	L	HD	J	H	K	L	HD	J	H	K	L
142	4.803	4.542	4.466	4.428	80170	3.400	2.810	2.684	2.596	165978	4.677	4.083	3.965	3.876
469	4.986	4.543	4.443	4.388	82074	–	–	–	–	166599	4.071	3.588	3.484	3.390
645	4.183	3.675	3.566	3.497	82734	3.396	2.926	2.812	2.727	169233	3.485	2.811	2.674	2.534
3303	4.325	3.748	3.632	3.557	85655	–	–	–	–	170525	–	–	–	–
6269	4.657	4.146	4.046	3.982	90170	–	–	–	–	172223	4.581	4.004	3.859	3.732
8779	4.335	3.650	3.513	3.408	92588	–	–	–	–	173902	4.827	4.272	4.148	4.041
9562	4.664	4.368	4.298	4.271	94386	–	–	–	–	177389	3.813	3.335	3.233	3.153
10142	4.226	3.673	3.570	4.475	99491	–	–	–	–	177565	–	–	–	–
11332	4.529	4.025	4.924	3.837	100219	–	–	–	–	188512	–	–	–	–
12583	4.282	3.821	3.716	3.656	104055	–	–	–	–	191067	4.240	3.729	3.621	3.541
13421	4.675	4.415	4.355	4.320	104307	–	–	–	–	194433	4.670	4.183	4.068	3.997
16589	5.573	5.321	5.265	5.231	100219	–	–	–	–	195564	4.417	4.097	4.021	3.971
18262	5.144	4.941	4.886	4.861	107773	–	–	–	–	196755	–	–	–	–
18907	4.362	3.899	3.811	3.752	120237	–	–	–	–	199223	4.540	4.098	3.992	3.919
19826	4.773	4.295	4.192	4.142	121056	–	–	–	–	200011	5.497	5.161	5.079	5.029
26913	5.737	5.401	5.330	5.270	121384	–	–	–	–	200073	4.084	3.493	3.362	3.280
26923	5.281	5.003	4.945	4.906	125184	–	–	–	–	202773	4.677	4.099	3.998	3.930
27442	2.710	2.198	2.079	2.005	126400	–	–	–	–	210434	4.437	3.952	3.843	3.776
29613	3.710	3.073	2.965	2.887	126868	–	–	–	–	211391	2.630	2.150	2.045	1.960
30608	4.553	3.637	3.859	3.772	140301	–	–	–	–	212330	4.176	3.837	3.751	3.696
34642	3.144	2.628	2.524	2.448	144585	–	–	–	–	214599	4.647	4.123	4.016	3.962
36553	4.446	4.183	4.110	4.077	145148	–	–	–	–	216385	4.292	4.021	3.965	3.922
37501	4.850	4.409	4.316	4.267	147723	–	–	–	–	216437	4.949	4.648	4.576	4.534
39937	4.633	4.223	4.116	4.055	152781	–	–	–	–	216718	4.248	3.770	3.670	3.598
40105	4.986	4.533	4.437	4.404	154556	–	–	–	–	217107	4.970	4.637	4.559	4.518
41700	5.427	5.175	5.116	5.084	155974	–	–	–	–	217703	4.347	3.850	3.752	3.690
50806	4.812	4.470	4.399	4.377	156846	–	–	–	–	219834	3.873	3.513	3.436	3.387
51825	5.424	5.201	5.150	5.114	157347	5.150	4.802	4.729	4.685	223524	4.077	3.524	3.402	3.322
62644	3.728	3.343	3.258	3.218	160691	4.033	3.693	3.610	3.558	224022	5.069	4.768	4.714	4.689
66011	5.273	4.985	4.909	4.861	165438	–	–	–	–	224750	4.909	4.460	4.358	4.299
72954	4.991	4.545	4.458	4.423										

for six stars only). For the two most rapid rotators in the sample (HD 16589 and HD 51825) we were not able to get reliable estimates of the EWs and metallicity was inferred by carrying out a complete spectral synthesis analysis. The same line parameters used for the EWs analysis, same model atmospheres, and our own synthetic code described in Gratton & Sneden (1990) were employed.

The sources of internal errors in the estimated Fe abundances are as follows: 0.028 dex are due to errors in EWs, 0.072 dex for ± 100 K uncertainty in T_{eff} , 0.030 dex for ± 0.3 dex in $\log g$, and 0.035 dex for ± 0.3 km s $^{-1}$ in ξ , giving a total error of 0.090 dex. Systematic errors are more difficult to evaluate; since we carried out a differential analysis with respect to the Sun, we estimate that they should not be larger than 0.1 dex and they should be dominated by possible errors in the effective temperatures scale.

Our resolution allowed us to separate the lithium 6707.8 Å line from the nearby 6707.441 Å blend in the spectra of slow rotators; for these stars we could measure the EWs of the Li 6707.8 Å alone and use them to derive Li abundances. Specifically, $\log n(\text{Li})$ were determined using the same model atmospheres which we employed to determine [Fe/H] assum-

ing the metallicity found in the previous step. A full spectral synthesis analysis was carried out for HD 16589, HD 41700, HD 51825, HD 66011, and HD 126868, the only stars in our sample where the Fe I blend could not be separated from the lithium doublet. Lithium equivalent widths, $\log n(\text{Li})$ and [Fe/H] values are given in Columns 4–6 of Table 3.

The errors in $\log n(\text{Li})$ values come from errors in measured equivalent widths and uncertainties in the inferred stellar parameters, T_{eff} , surface gravity, and microturbulence. Given the high S/N of our spectra, errors in EWs are negligible in most cases and, in any case, the largest errors come from the uncertainty in T_{eff} . We estimate that an error of ± 100 K would result in $\Delta \log n(\text{Li}) \pm 0.15$ dex, while both an error of 0.3 dex in $\log g$ and of 0.3 km s $^{-1}$ in ξ would produce a negligible error in $\log n(\text{Li})$.

We have searched through the literature for previous determinations of lithium and/or iron abundances for our sample stars, finding $\log n(\text{Li})$ determinations for 13 stars (from various sources) and [Fe/H] for 24 stars (from Cayrel de Strobel et al.'s catalogue, 1997). In Fig. 1 we compare $\log n(\text{Li})$ (panel a) and [Fe/H] (panel b) values derived by us with those from the literature. The figure shows a very good agreement for \log

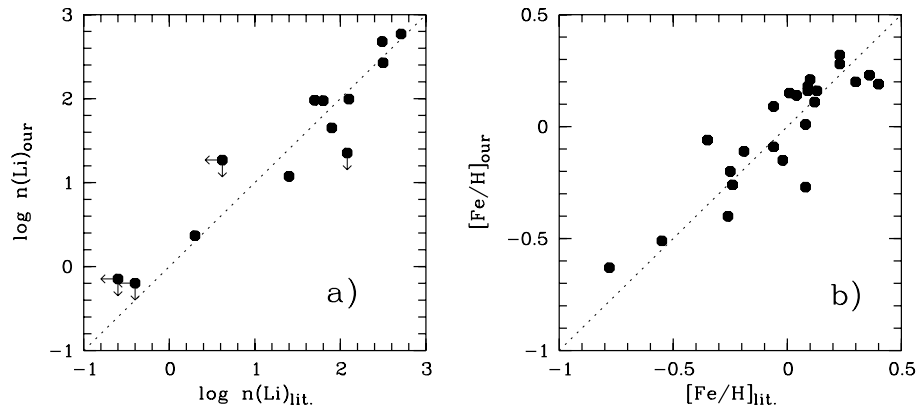


Fig. 1. **a** $\log n(\text{Li})$ inferred in the present work vs. $\log n(\text{Li})$ from the literature (Duncan 1981; Pallavicini et al. 1987; Balachandran 1990; Soderblom et al. 1993; Pasquini et al. 1994; Favata et al. 1995, 1997). **b** Same as panel **a** but $[\text{Fe}/\text{H}]$ values are compared. $[\text{Fe}/\text{H}]$ values from the literature come from the catalogue of Cayrel de Strobel et al. (1997).

$n(\text{Li})$ values. If we exclude upper limits, that are obviously different due to different resolution and S/N ratios, for the majority of the stars the differences in $\log n(\text{Li})$ are very small. In most cases the differences are due to the assumed effective temperatures. The only significantly discrepant point is HD 13421 (HR 635). This star has been observed by Balachandran (1990) who gives an equivalent width of 14 mÅ for the lithium feature. Our spectrum does not exhibit the $\lambda 6707.8$ lithium line and we were able to infer only an upper limit of 3 mÅ to its equivalent width. Panel b) of the figure evidences a larger scatter; in a few cases the difference between our values and the ones from the literature is larger than our internal error of 0.09 dex, but no systematic shifts seem to be present. One of the reasons for the discrepancies could be that some of the Cayrel et al. $[\text{Fe}/\text{H}]$ determinations have been taken from rather old papers with possibly less accurate metallicity determinations (due to the worse data quality). The most discrepant star is HD 62644 for which we derived $[\text{Fe}/\text{H}] = -0.06$, while Cayrel de Strobel et al. quote $[\text{Fe}/\text{H}] = -0.35, -0.22, -0.21$ (from Hearnshaw 1972; Gratton & Sneden 1991, 1994); as far as Gratton & Sneden results are concerned, the difference between the metallicities inferred by them and by us is due to the fact that we use a 181 K larger T_{eff} and measured slightly different EWs. Note that the $[\text{Fe}/\text{H}]$ value derived by us is more consistent with the value inferred from Strömberg photometry ($[\text{Fe}/\text{H}] = +0.01$).

The distribution of $[\text{Fe}/\text{H}]$ values is shown in Fig. 2. The distribution peaks around solar metallicities, but a significant dispersion is present. About 70% of the stars have $[\text{Fe}/\text{H}]$ typical of disk stars ($-0.2 < [\text{Fe}/\text{H}] \leq 0.2$), about 20% are somewhat metal poor (the most metal poor star has $[\text{Fe}/\text{H}] = -0.79$), and the remaining 10% have $[\text{Fe}/\text{H}] > 0.2$.

4.3. Masses and ages

Masses and ages were derived using Bertelli (1998) evolutionary tracks (see also Bertelli et al. 1994), assuming that all stars have not yet ignited He. Specifically, a linear interpolation (extrapolation) within the tracks for different metallicities was carried out: for stars with $[\text{Fe}/\text{H}] < 0$ the $z = 0.008$ ($[\text{Fe}/\text{H}] = -0.4$) and $z = 0.02$ ($[\text{Fe}/\text{H}] = 0$) tracks were used, while for stars with metallicity larger than solar the interpolation was carried out between the $z = 0.02$ and $z = 0.05$ ($[\text{Fe}/\text{H}] = +0.4$) tracks.

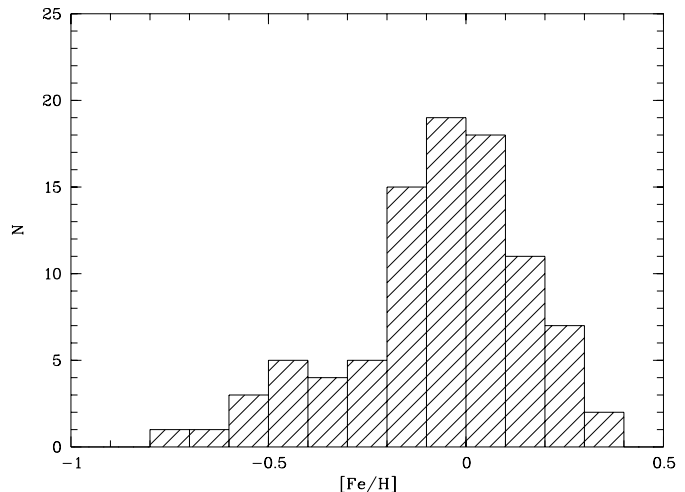


Fig. 2. Histogram of the metallicity ($[\text{Fe}/\text{H}]$) distribution of our sample stars.

In interpolating tracks, we neglected the possibility that a star could be in the short phase between the red and blue hook on the MS. The inferred masses and ages are listed in the last two columns of Table 3. Note that in the following discussion we will make extensive use of masses, but not of ages directly; they are however listed in the table for sake of completeness. Masses and ages were not derived for stars with $M_V < 1$, due to possible confusion with He-burning phases, nor for stars whose position in the color magnitude diagram was not reproducible by any track. In addition, we were unable to give an estimate of the age for three stars in our sample which lie right on the Zero Age Main Sequence for their measured $[\text{Fe}/\text{H}]$ ¹; namely, HD 26913, HD 26923, and HD 41700. Information on age for these stars, based on the Ca II H & K lines fluxes, is available from the literature (Soderblom et al. 1993; Duncan 1984) according to which, they are all MS stars younger than 10^9 years. For this reason we exclude them from the following discussion².

¹ Bertelli et al. tracks assume the following relation $Y = 0.23 + 2.5 Z$ between helium and metal contents.

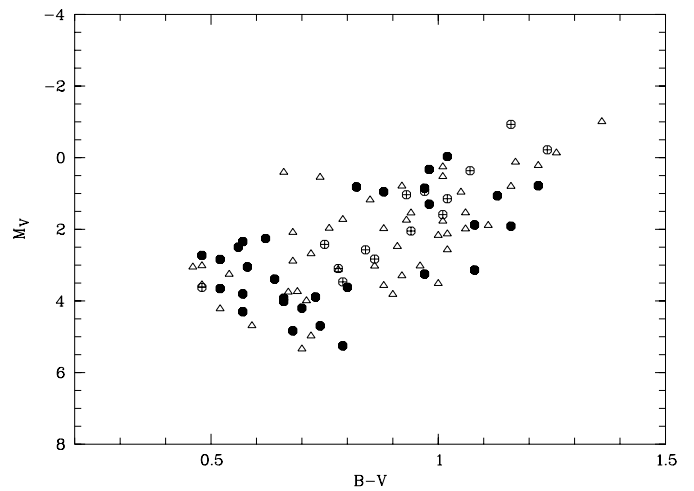
² Although we have mentioned that MS stars might be present in the sample, we want to be sure that they are old MS stars, i.e., that their lithium content has already undergone the phase of MS depletion.

Table 3. The inferred parameters

HD #	T_{eff} (K)	logg	EW (Li) (mÅ)	log n(Li)	[Fe/H]	log age (yrs)	M (M_{\odot})
142	6170	4.2	57	+2.780	+0.07	9.5	1.2
469	5298	2.6	14	+1.195	-0.03
645	4833	3.0	7	+0.326	-0.00	9.2	1.8
3303	4700	2.7	≤ 6	$\leq +0.084$	-0.41	9.7	1.2
6269	4872	2.8	≤ 6	$\leq +0.307$	-0.39	9.1	1.8
8779	4325	1.8	≤ 4	≤ -0.658	-0.40
9562	5825	3.9	62	+2.530	+0.18	9.7	1.2
10142	4739	2.5	≤ 3	≤ -0.170	-0.09
11332	4894	2.3	≤ 3	$\leq +0.029$	+0.02
12583	4955	2.6	≤ 7	$\leq +0.478$	+0.09
13421	6100	3.8	≤ 3	$\leq +1.278$	+0.23	9.5	1.5
16589	6194	3.9	-	$\leq +1.400$	+0.15	9.4	1.4
18262	6438	4.0	7	+1.922	+0.32	9.1	1.6
18907	5081	3.6	≤ 10	$\leq +0.791$	-0.63	9.9	1.0
19826	4934	3.1	13	+0.731	-0.09	9.1	1.9
26913	5634	4.6	66	+2.384	+0.01	...	1.0
26923	5980	4.5	88	+2.918	-0.02	...	1.1
27442	4749	3.3	≤ 3	≤ -0.157	+0.22	10.	1.2
29613	4656	2.7	≤ 5	≤ -0.056	-0.26	9.8	1.2
30608	4622	2.2	≤ 3	≤ -0.331	-0.34
34642	4811	3.1	≤ 2	≤ -0.254	-0.15	9.5	1.4
36553	5964	3.7	≤ 5	$\leq +1.389$	+0.32	9.4	1.6
37501	5132	3.0	≤ 2	$\leq +0.139$	-0.17	8.9	2.2
39937	5432	2.6	-	$\leq +1.136$	-0.00
40105	5034	3.7	29	+1.227	-0.06	9.9	1.1
41700	6180	4.4	-	+2.923	-0.01	...	1.2
50806	5578	4.0	11	+1.377	-0.02	9.9	1.0
51825	6445	4.1	-	+2.600	-0.15	9.2	1.4
62644	5365	3.7	≤ 4	$\leq +0.706$	-0.06	9.6	1.3
66011	6025	3.7	-	$\leq +2.000$	+0.25	9.4	1.5
72954	5204	3.4	≤ 2	$\leq +0.222$	-0.42	9.3	1.5
80170	4537	2.1	8	-0.016	-0.02
82074	5055	3.3	≤ 2	$\leq +0.047$	-0.48	9.4	1.4
82734	4897	2.2	44	+1.333	+0.19
85655	4254	1.4	94	+0.842	-0.10
90170	5029	3.2	34	+1.359	-0.15	9.2	1.8
92588	5044	3.6	≤ 2	$\leq +0.034$	-0.10	9.8	1.1
94386	4545	2.7	≤ 4	≤ -0.315	+0.08	10.	1.1
99491	5338	4.4	≤ 3	$\leq +0.549$	+0.16	9.8	1.0
100219	6124	4.0	≤ 4	$\leq +1.425$	+0.02	9.4	1.3
104055	4396	1.9	7	-0.290	-0.01
104307	4451	2.0	9	-0.091	-0.01
107773	4870	3.3	≤ 2	≤ -0.179	-0.51	9.8	1.1
114837	6191	4.2	26	+2.335	-0.40	10.	1.3
120237	6021	4.4	≤ 2	$\leq +1.034$	+0.09	9.1	1.2
121056	4711	3.0	≤ 2	≤ -0.386	-0.11	9.5	1.4
121384	5181	3.6	6	+0.681	-0.51	9.6	1.2
125184	5533	4.0	≤ 2	$\leq +0.576$	+0.16	9.9	1.1
126400	4814	3.0	≤ 2	≤ -0.250	-0.32	9.5	1.4
126868	5521	3.3	-	+2.643	-0.06	9.2	1.8
140301	4494	2.3	≤ 2	≤ -0.708	-0.17
144585	5778	4.1	13	+1.647	+0.28	9.8	1.1
145148	4768	3.4	4	-0.004	-0.07	10.	1.1
147723	5929	3.8	28	+2.145	+0.10	-	-
152781	4982	3.6	9	+0.623	-0.00	9.6	1.3
154556	4713	2.9	3	-0.205	+0.04	9.5	1.4

Table 3. (continued)

HD #	T_{eff} (K)	logg	EW (Li) (mÅ)	log n(Li)	[Fe/H]	log age (yrs)	M (M_{\odot})
155974	6265	4.0	46	+2.724	-0.11	9.9	+9
156846	5989	3.9	≤ 2	$\leq +1.007$	+0.11	9.5	1.4
157347	5659	4.4	≤ 2	$\leq +0.703$	+0.05	9.6	1.0
160691	5668	4.2	≤ 4	$\leq +1.015$	+0.20	9.9	1.1
165438	4862	3.4	4	+0.115	+0.02	9.5	1.4
165978	4660	2.6	9	+0.211	-0.37	9.5	1.4
166599	5005	2.6	≤ 2	≤ -0.013	-0.03
169233	4341	1.5	≤ 2	≤ -0.960	-0.79
170525	5535	3.7	≤ 2	$\leq +0.578$	-0.20	9.5	1.3
172223	4532	2.3	42	+0.791	+0.29
173902	4678	2.9	7	+0.123	+0.10	9.4	1.5
177389	5018	3.4	8	+0.614	-0.11	9.3	1.6
177565	5519	4.4	≤ 2	$\leq +0.562$	+0.01	9.7	1.0
188512	5097	3.5	≤ 2	$\leq +0.097$	-0.27	9.6	1.3
191067	4759	3.1	≤ 3	≤ -0.037	-0.13	9.9	1.1
194433	4916	3.5	30	+1.156	+0.09	9.5	1.4
195564	5614	4.0	33	+1.970	+0.02	9.9	1.1
196755	5510	3.6	14	+1.418	-0.09	9.5	1.4
199223	5113	2.6	≤ 2	$\leq +0.116$	+0.13
200011	5652	3.5	≤ 2	$\leq +0.696$	-0.09	9.3	1.6
200073	4569	2.7	≤ 3	≤ -0.409	-0.15	10.	1.1
202773	4714	2.5	3	-0.203	-0.59
210434	4928	3.0	≤ 4	$\leq +0.197$	+0.09	8.8	2.4
211391	4968	2.4	≤ 4	$\leq +0.246$	+0.15
212330	5653	4.0	17	+1.652	-0.04	9.9	1.1
214599	4812	2.4	22	+0.820	-0.14
216385	6250	4.0	≤ 2	$\leq +1.221$	-0.20	9.5	1.3
216437	5781	4.1	26	+1.976	+0.21	9.8	1.1
216718	5071	2.7	28	+1.254	+0.14
217107	5597	4.3	≤ 2	$\leq +0.641$	+0.30	10	1.0
217703	4897	3.0	27	+1.025	-0.20	9.2	1.8
219834	5495	3.9	49	+2.078	+0.09	9.8	1.1
223524	4609	4.2	≤ 3	≤ -0.350	+0.07	9.2	1.7
224022	6021	3.3	61	+2.689	+0.12	9.5	1.2
224750	5217	3.5	≤ 2	$\leq +0.237$	-0.17	9.2	1.8

**Fig. 3.** Color-magnitude diagram of our sample stars. Filled symbols denote stars with $[\text{Fe}/\text{H}] > 0.05$, triangles indicate stars with $-0.3 < [\text{Fe}/\text{H}] \leq 0.05$, and crossed circles indicate stars with $[\text{Fe}/\text{H}] \leq -0.3$.

5. Discussion

5.1. Different stellar populations in the sample

In Fig. 3 we show the $B-V$ vs. M_V color–magnitude diagram for our sample stars. The sample has been divided in three metallicity groups; namely, $[\text{Fe}/\text{H}] \leq -0.3$ (crossed circles, group (a)), $-0.3 < [\text{Fe}/\text{H}] \leq 0.05$ (open triangles, group (b)), and $[\text{Fe}/\text{H}] > 0.05$ (filled circles, group (c)). The figure shows that for all metallicities stars with $M_V < 1$, i.e., evolved giants, are present. The subgiant branch is very well defined by the 14 stars in group (a), while it is very dispersed for stars in group (b), evidencing the spread in age and mass which appears from Table 3. On the other hand, whereas only one star in group (a) is close to the MS, a fraction of stars in groups (b) and, particularly, (c), are very close to it. It is likely that some of the metal-rich stars are actually MS stars rather than subgiants; as we have mentioned, our sample has been selected on the basis of spectral type, but for metal-rich dwarfs there is a tendency to underestimate the spectral class since the MS becomes more luminous. We finally note that the C-M diagram for stars in group (c) exhibits an evident Hertzsprung gap, and that, among evolved stars, six objects are present that seem to define the He central burning clump. To summarize, our sample contains stars belonging to different stellar populations and in very different evolutionary stages; a large percentage of subgiants are included in it, but some MS stars as well as first ascent giants and, possibly, He clump objects are also present.

5.2. Li abundances in the C-M diagram

In Fig. 4 we show again the C-M diagram of our sample stars with symbols of different sizes indicating different lithium abundances. Stars in groups (a), (b), (c) as defined in the previous section are plotted in the bottom, middle, and top panels, respectively. Known binaries and/or active stars are indicated as filled circles, while supposedly single stars are plotted as open symbols. β Hyi is also plotted in the middle panel (star symbol). The 1, 3, and 10 Gyrs isochrones of Bertelli (1998) for $z = 0.008$, $z = 0.02$, and $z = 0.05$ are superimposed in the three panels (from bottom to top, respectively).

A first, qualitative look at Fig. 4 indicates that, as expected, most of the evolved stars have a low lithium content and at least a part of the evolved stars with high lithium ($\log n(\text{Li}) \geq 1$) are binaries or known active stars. Several papers in the last few years have addressed the problem of lithium in close binaries and chromospherically active stars (e.g., Pallavicini et al. 1987; Fekel & Balachandran 1993; Fernandez-Figueroa et al. 1993; Randich et al. 1993, 1994; Pallavicini & Randich 1994 and references therein; Barrado y Navascués et al. 1997, 1998); all of these papers agreed that active binaries tend to be more lithium rich than inactive stars of the same spectral type, albeit higher than normal lithium is not a characteristics of all active binaries. Our sample, which has not been selected on the basis of activity and/or binarity, indeed confirms this result. Although in the following we will mention again about the binarity–lithium relation, a throughout investigation of the reasons why active

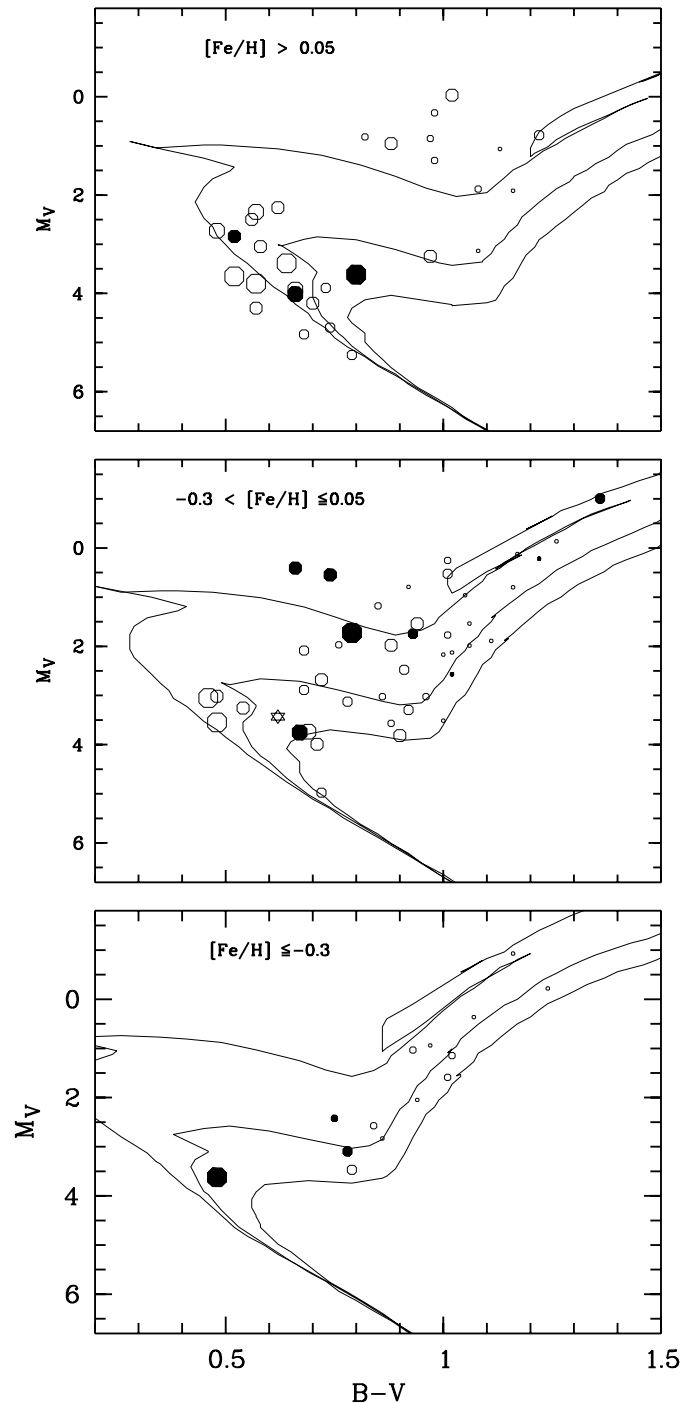


Fig. 4. Color-magnitude diagrams for stars with $[\text{Fe}/\text{H}] > 0.05$ (top panel), $-0.3 < [\text{Fe}/\text{H}] \leq 0.05$ (middle panel), and $[\text{Fe}/\text{H}] \leq -0.3$ (bottom panel). Different symbol sizes denote stars with different lithium abundances; namely, from the smallest to the largest symbols, $\log n(\text{Li}) \leq 0$, $0 < \log n(\text{Li}) \leq 0.5$, $0.5 < \log n(\text{Li}) \leq 1$, $1 < \log n(\text{Li}) \leq 1.5$, $1.5 < \log n(\text{Li}) \leq 2$, $2 < \log n(\text{Li}) \leq 3$, and $\log n(\text{Li}) > 3$. Open and filled symbols represent supposedly single stars and binaries, respectively; β Hyi is shown as a star symbol in the middle plot. The 1, 3, and 10 Gyr isochrones of Bertelli (1998) for $z = 0.05$ (top), $z = 0.02$ (middle), $z = 0.008$ (bottom) are also shown in the three panels.

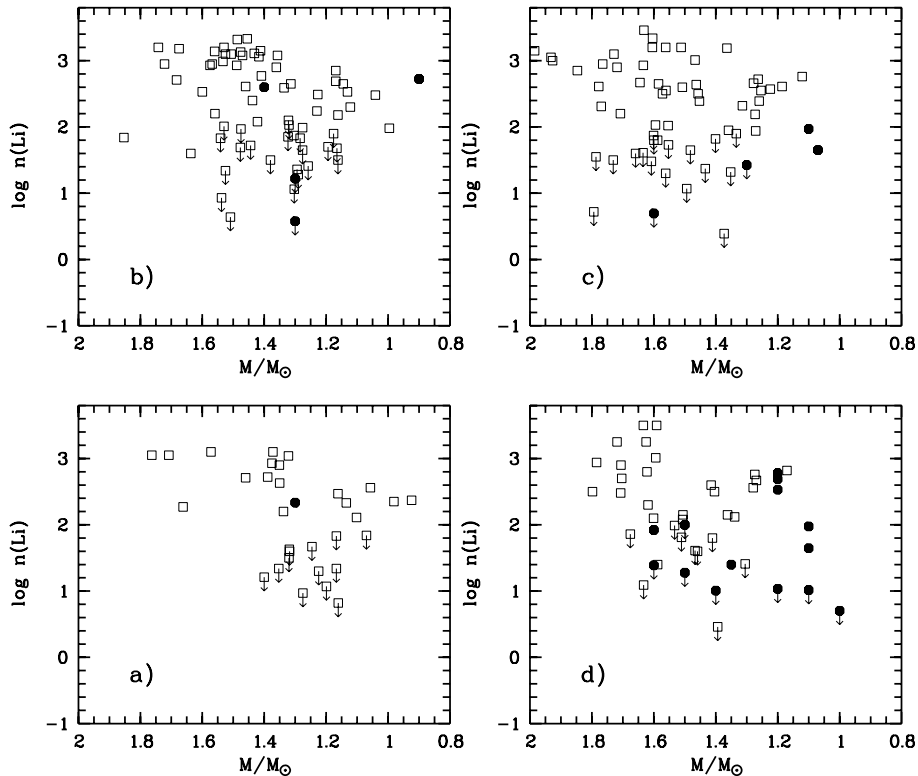


Fig. 5a–d. $\log n(\text{Li})$ vs. mass distribution for stars that have not yet undergone first dredge-up dilution. The stars have been subdivided in four metallicity bins: $[\text{Fe}/\text{H}] \leq -0.3$ (panel a), $-0.3 < [\text{Fe}/\text{H}] \leq -0.1$ (panel b), $-0.1 < [\text{Fe}/\text{H}] \leq 0.05$ (panel c), and $0.05 < [\text{Fe}/\text{H}]$ (panel d). Stars in the Balachandran (1990) sample (open squares) and stars in the present sample (filled circles) are plotted. In the latter, only stars bluer than $B-V=0.7$ are considered (see Sect. 5.4).

binaries seem to have a different lithium evolution is beyond the purposes of the present paper.

Fig. 4 in addition indicates that: *i*) a one-to-one correspondence between lithium abundance and position in the diagram is not evident, although an average decrease of lithium is clear going from the left side to the right side of the diagram. For solar and over-solar metallicity stars a significant spread in lithium is present both among slightly evolved stars and for stars in the Hertzsprung gap; *ii*) lithium destruction seems to be rather fast once a star has evolved away from the turn-off; on the other hand, there does not seem to be considerable variation in Li abundance from the MS to the TO or red hook (i.e., during the earliest phases of evolution out of the MS); a few β Hyi-like stars, i.e., slightly evolved stars with high lithium ($\log n(\text{Li}) > 2$) are present in the sample, as well as stars in a similar evolutionary stage, but showing a larger Li depletion; *iii*) although a dispersion in lithium is present along the whole subgiant branch, a drop of the average lithium content is evident for stars later than $B-V \sim 0.9$, qualitatively witnessing the second mixing, or extra-mixing episode. In the following we will address the above points in greater detail.

5.3. Early-stages of evolution out of the MS

5.3.1. Lithium vs. mass

Before addressing the issue of the evolution of lithium abundance along the subgiant branch, we wish to briefly recall the main results of Balachandran (1990) regarding the distribution of $\log n(\text{Li})$ among stars that have just left the MS, i.e., the pro-

genitors of the stars in the more advanced phases of the subgiant branch. In so doing, we take advantage of the fact that we are able to derive masses for these stars (in the same way as it was done for our sample stars). We show in Fig. 5 $\log n(\text{Li})$ vs. mass for the stars in the sample of Balachandran (open squares) complemented by the stars in our sample with $B-V$ lower than 0.7 (i.e., those that have not yet undergone first dredge-up dilution – filled circles). Four metallicity bins were considered: $[\text{Fe}/\text{H}] \leq -0.3$ (panel a), $-0.3 < [\text{Fe}/\text{H}] \leq -0.1$ (panel b), $-0.1 < [\text{Fe}/\text{H}] \leq 0.05$ (panel c), and $[\text{Fe}/\text{H}] > 0.05$ (panel d). The main points to be noticed in the figure are: 1. the large scatter in $\log n(\text{Li})$ that characterizes stars of all masses and metallicities; 2. the lithium ‘dip’ (e.g., Boesgaard and Tripicco 1986; Balachandran 1995 and references therein) is evident in all the four panels. The position of the center of the dip varies with metallicity, from about $1.25 M_{\odot}$ for low-metallicity stars to about $1.5 M_{\odot}$ for stars with $[\text{Fe}/\text{H}] > 0.05$. The dip in the Hyades is centered at $1.4 M_{\odot}$ (e.g., Balachandran 1995). Note that the dip among field stars is not as sharp and well delineated as in the Hyades, due to the large scatter in lithium among stars of both higher and lower masses; 3. several F-type, relatively massive stars outside the lithium ‘dip’ show significant Li destruction.

5.3.2. The case of β Hyi

Did β Hyi dredge-up previously stored lithium? In order to address this question, a sample of solar-like stars (i.e., stars that are still on the MS, with masses around $1 M_{\odot}$) and a sample of β Hyi-like stars (i.e., stars, with similar masses, that have already left the MS, but that have not yet undergone significant post-MS

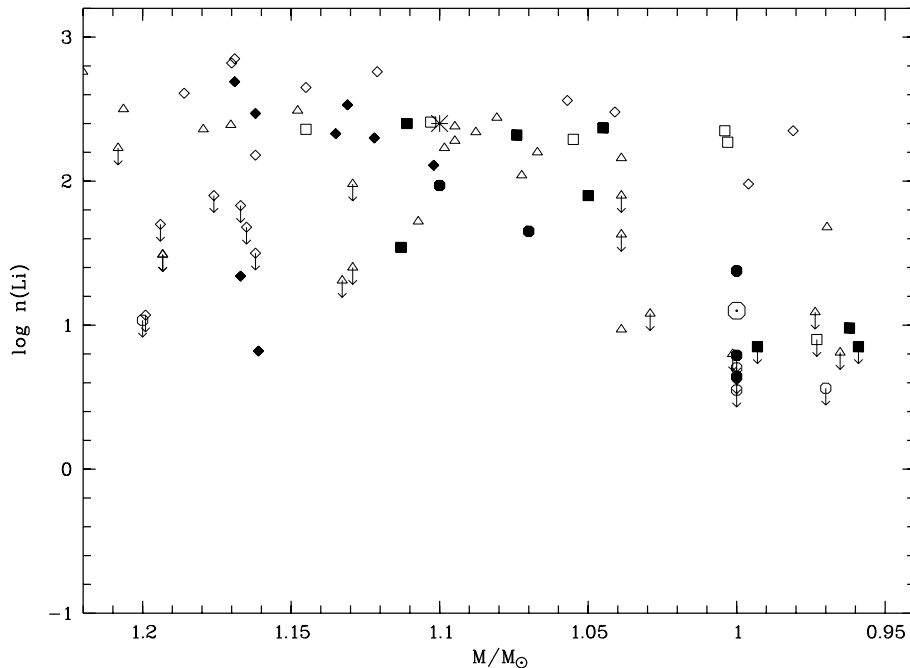


Fig. 6. $\log n(\text{Li})$ vs. mass for stars in the present sample (circles), Balachandran (1990, diamonds), Pasquini et al. (1994, squares), M67 (triangles). Filled and open symbols represent, respectively, slightly evolved and non-evolved stars as defined in the text. The Sun and β Hyi (asterisk) are also plotted.

evolution) should be compared. We show such a comparison in Fig. 6, where we plot $\log n(\text{Li})$ vs. mass for slightly evolved and unevolved stars in a narrow mass range ($0.95 \leq M \leq 1.25 M_{\odot}$). Evolved, or β Hyi-like, stars are indicated in the figure as filled symbols, while open symbols denote MS stars. Squares and circles indicate stars in Pasquini et al.'s (1994) and the present samples, respectively. Diamonds indicate stars in the sample of Balachandran (1990) and open triangles indicate M67 data from Pasquini et al. (1997). In order not to bias the results, we excluded from the sample of Pasquini et al. likely young stars as indicated from their chromospheric activity level (stars with a Ca II K line flux $-\log F'_{K}$ larger than $5.7 \text{ erg cm}^{-2} \text{ s}^{-1}$). The subdivision non-evolved/slightly-evolved was done on the basis of the location of the stars on the C-M diagram; namely, we considered as slightly evolved the stars that are redder than the turn-off, but bluer than $B-V = 0.7$ (see Sect. 5.4 below). β Hyi (symbol = asterisk) and the Sun are also plotted in the figure. The figure suggests that the distributions of abundances for slightly evolved and unevolved stars are rather similar. Both groups show a large dispersion in abundance with several stars having lithium comparable to or slightly higher/lower than β Hyi and as many stars with a very low lithium content. Neither the Sun nor β Hyi appear as peculiar objects in the figure. On the contrary, if the mechanism proposed by Dravins et al. (1993) to explain the high lithium content of β Hyi were at work, one would expect that, on average, stars in the same evolutionary status as β Hyi should show systematically higher lithium than stars in the same evolutionary status as the Sun. Fig. 6 suggests that this is not the case and, in particular that several solar-mass slightly evolved stars have a very low lithium content.

We conclude that, before significant dilution occurs (see next sections), the Li distribution of stars that have just evolved off the MS closely resembles that of stars still on the MS and

that β Hyi-like stars are most likely the descendants of old MS stars which did not destroy a large amount of lithium, rather than stars which left the MS with an apparently low lithium content and then dredge it up as soon as they evolve off the MS.

5.4. Li evolution along the subgiant branch

Plotted in Fig. 7 is $\log n(\text{Li})$ vs. $B-V$; all stars in our sample redder than the turnoff and fainter than $M_V = 1$ are considered. Different symbols indicate stars with different metallicities: namely, triangles, squares and circles denote stars with $[\text{Fe}/\text{H}] \leq -0.3$, $-0.3 < [\text{Fe}/\text{H}] \leq 0.05$, and $[\text{Fe}/\text{H}] > 0.05$, respectively. The sample of Balachandran (1990, open symbols) has again been combined with ours (filled circles), since it is representative of the $\log n(\text{Li})$ distribution of the progenitors of our sample stars. Under the assumption that, at a given mass, the $B-V$ color can be regarded as an indicator of the evolution along the subgiant branch, the figure permits us to follow such an evolution as far as lithium is concerned. The figure shows that for all metallicities first dredge-up dilution is completed for stars later than $B-V \sim 0.7$, or $T_{\text{eff}} \sim 5600\text{--}5700 \text{ K}$ (according to our $T_{\text{eff}}\text{--}B\text{--}V$ calibration); such a value is similar to what observed by Pilachowski et al. (1993) for population II subgiants, indicating that the color where complete Li dilution occurs does not depend much on either mass or metallicity. Interestingly, the only two stars with $B-V$ greater than 0.7 and $\log n(\text{Li})$ larger than 1.5 are a spectroscopic binary (HD 219834) and a very active star (HD 126868), suggesting that binarity and/or rapid rotation may in some way affect first dredge-up dilution. Fig. 7 also exhibits a large spread in Li, with only a minority of the stars that have undergone dilution having abundances close to $\log n(\text{Li}) \sim 1.5\text{--}1.8$, the value predicted by first dredge-up computations; many of the stars indeed have $\log n(\text{Li})$ signif-

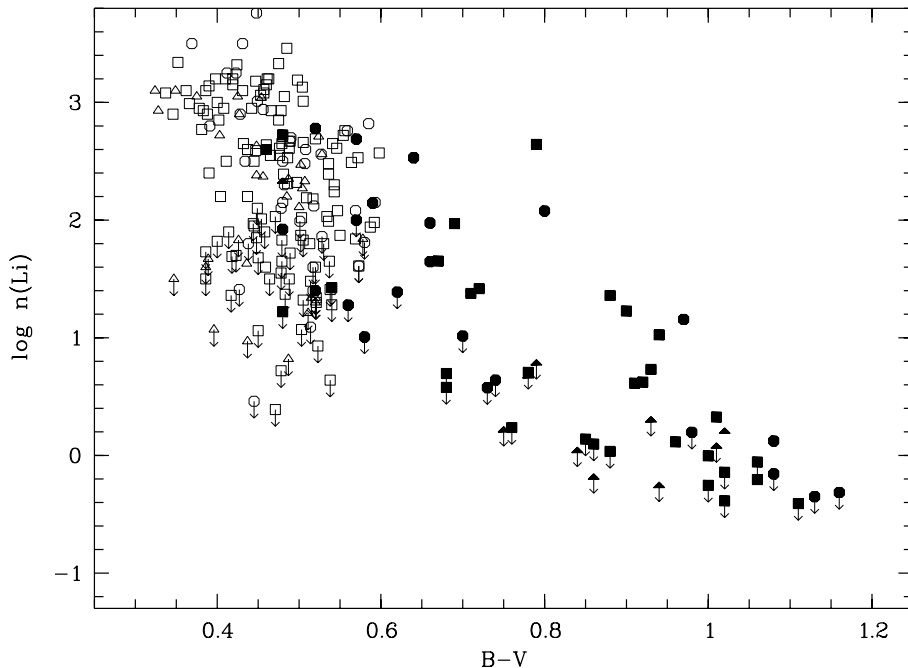


Fig. 7. $\log n(\text{Li})$ vs. $B-V$ color for all stars in our sample with $M_V > 1$ (filled symbols) and for stars in the sample of Balachandran (1990 – open symbols). The stars have been divided in the metallicity bins defined in Sect. 5.1; stars in groups (a) ($[\text{Fe}/\text{H}] \leq -0.3$), (b) ($-0.3 < [\text{Fe}/\text{H}] \leq 0.05$), and (c) ($[\text{Fe}/\text{H}] > 0.05$) are plotted as triangles, squares, and circles.

icantly below 1. At variance with Pop. II stars which have a uniform Li abundance when they leave the MS, it is difficult to give an exact estimate of the amount of dilution for our sample stars and to discern whether the diluted lithium content is consistent with theoretical predictions. As we have shown in the previous sections and as Fig. 7 itself indicates, Pop. I stars at the end of their MS permanence are characterized by a spread in lithium, with several stars showing severe Li depletion. Consequently, a dispersion in $\log n(\text{Li})$ among stars that have passed the first dredge-up is expected, and finding stars with a very low lithium is neither surprising nor it necessarily means a larger than expected dilution/depletion during first dredge-up. More quantitatively, 36 and 87 out of the 188 stars in the sample of Balachandran (1990), i.e., ~ 20 and 45% of them, have $\log n(\text{Li}) \geq 3$ and 2.5, respectively; considering a dilution factor of about 60, $\log n(\text{Li}) \sim 3$ and 2.5 would correspond to diluted $\log n(\text{Li}) \sim 1.3$ and 0.7. We find that 12 and 44% of the stars in our sample with $0.7 \leq B-V \leq 0.9$ (i.e., stars that have undergone the first dredge-up dilution, but have not passed the second mixing episode - see below) have $\log n(\text{Li}) \geq 1.3$ and 0.7, respectively. Given that neither Balachandran's nor our sample are complete and that the distributions in mass and metallicity of the two samples are not necessarily the same, the agreement between the observed and predicted lithium is rather good.

An additional feature to be noted in Fig. 7 is the drop of the upper envelope of the $\log n(\text{Li})$ vs. $B-V$ distribution which occurs at $B-V \sim 0.9-0.95$ and which is indicative of a second mixing episode. In order to investigate this issue in more detail, we show in Fig. 8 $\log n(\text{Li})$ vs. absolute bolometric magnitudes M_{bol} , that have been inferred from M_V and BC from Kurucz (1993 – see Sect. 4.1). Only stars with $B-V$ larger than 0.7 are considered in the figure; evolved giants with $M_V < 1$ are again not taken into account. Symbols indicating different

metallicity groups are the same as in Fig. 7. The luminosity of the evolutionary point where extra-mixing is thought to occur which, we recall, corresponds to the point where the hydrogen burning shell crosses the chemical discontinuity created by the convective envelope at its maximum extent, depends on mass and metallicity (Charbonnel 1994). Accordingly, we subdivided our sample stars in two mass bins: in the bottom and top panels stars with masses above and below $1.4 M_{\odot}$ are displayed. The six lines in each panel indicate the expected M_{bol} where extra-mixing should take place as computed by Charbonnel (1994 – Table 3); the lines refer to different masses and metallicities, as explained in the figure caption.

Due to the spread in mass and metallicity among the stars in the two groups and to the limited sample sizes, it is not possible to give a precise estimate of the luminosity where extra-mixing actually occurs and, specifically, to tabulate such a luminosity as a function of mass and metallicity. Nevertheless, looking again at the upper envelope of the $\log n(\text{Li})$ vs. M_{bol} distribution in the two panels, it seems evident that extra-mixing becomes efficient at luminosities lower than those predicted by Charbonnel (1994). This is particularly the case for stars with masses below $1.4 M_{\odot}$. No stars are present in the upper panel with $M_{\text{bol}} < 2$ (or $\log L/L_{\odot} > 1.1$) and $\log n(\text{Li})$ larger than 1; therefore, $\log L/L_{\odot} \sim 1.1$ can be regarded as an upper limit to the luminosity of the point where extra mixing starts for stars with masses below $1.4 M_{\odot}$, at least as far as solar and over-solar metallicity stars are concerned. There are very few stars in the sample with $[\text{Fe}/\text{H}] < -0.3$ and virtually all of them are already severely depleted in lithium after the first dredge-up dilution; it is therefore difficult to constrain the magnitude where the second mixing episode occurs for these stars and we cannot exclude that it actually occurs at lower M_{bol} /higher luminosities. For stars with masses above $1.4 M_{\odot}$, the distribution of points

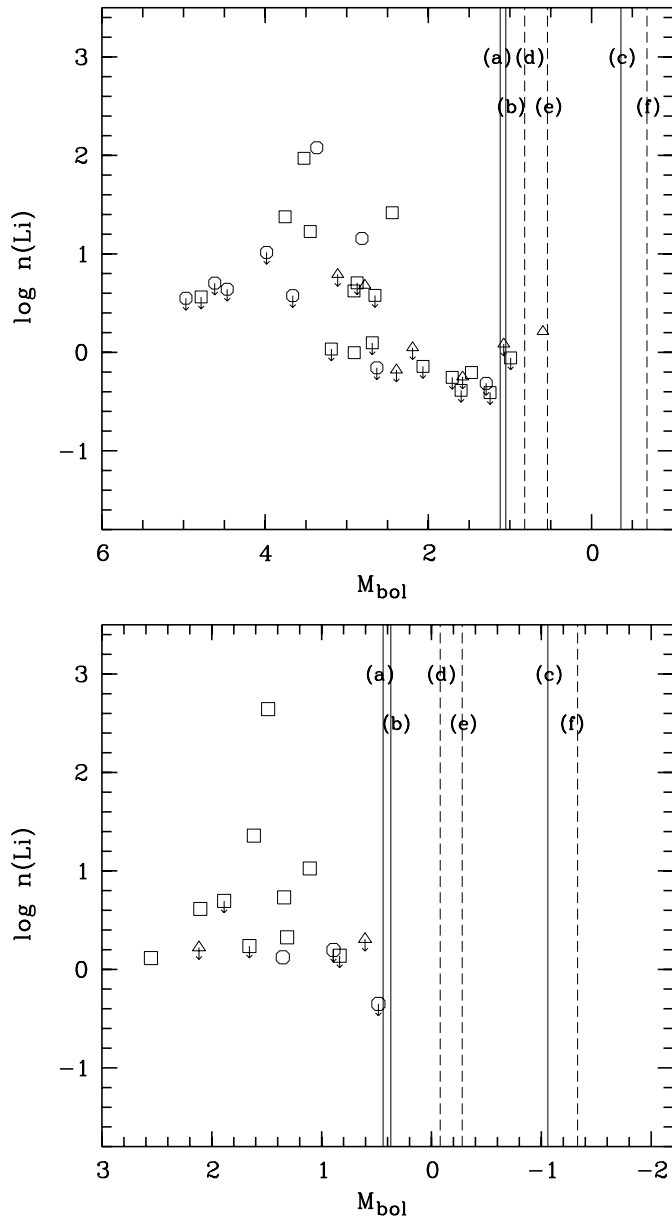


Fig. 8. $\log n(\text{Li})$ vs. absolute bolometric magnitude for stars in our sample with $B-V > 0.7$ (i.e., stars that have completed the first-dredge up dilution) and $M_V > 1$. Open triangles represent stars with $[\text{Fe}/\text{H}] \leq -0.3$, open squares stars with $-0.3 < [\text{Fe}/\text{H}] \leq 0.05$, and open circles stars with $[\text{Fe}/\text{H}] > 0.05$. Stars with masses above and below $1.4 M_\odot$ are shown in the bottom and top panel, respectively. The six vertical lines in each panel represent the position of the evolutionary point where extra-mixing should occur, as predicted by Charbonnel (1994). Solid curves labelled as (a), (b), (c) refer to $z = 0.05$, $z = 0.02$, and $z = 0.001$, respectively, and masses $M = 1$ (top panel) and $1.5 M_\odot$ (bottom panel). Dashed curves labelled as (d), (e), (f) refer to $z = 0.05$, $z = 0.02$, and $z = 0.001$, respectively, and masses $M = 1.25$ (top panel) and $1.7 M_\odot$ (bottom panel).

in the bottom panel of Fig. 8 suggests an upper limit to the extra-mixing episode luminosity $\log L/L_\odot \sim 1.5$ and the difference between the observed and predicted luminosities seems smaller

than for less massive stars (although the extra-mixing signature is not as evident as in the top panel).

At variance with our results, Carretta et al. (1998) found that, for their sample of Pop. II metal poor stars, extra-mixing occurs at $\log L/L_\odot \sim 2$ ($M_{\text{bol}} \sim -0.3$) in good agreement with the prediction of Charbonnel (1994). On the other hand, Bertelli (1998) models predict bolometric luminosities of the RGB bump (which corresponds to the point where the mixing episode occurs) which are fainter than those predicted by Charbonnel (1994) (by ~ 0.4 – 0.5 mag for $z=0.02$ and $z=0.05$) and in better agreement with the indications from our data. In conclusion, the above points and, specifically, the comparison of our results with those of Carretta et al. (1998), suggest that the dependence on metallicity and mass of the luminosity where extra-mixing occurs (L_{EM}) is stronger than predicted by the models, which seem to work fairly well for relatively high masses and/or low metallicities, but which fail to reproduce the results of lower masses and close to solar metallicities. Unfortunately, although our sample as a whole is considerably large, we end up having very few stars per mass/metallicity bin, which does not allow us to empirically constrain in a more quantitative way L_{EM} and to disentangle its mass and metallicity dependence. Additional observational and theoretical efforts should be undertaken in order to clarify this issue.

Sofar we have not considered stars with $M_V \leq 1$, both since we do not derive masses of these stars and since e.g., clump giants have rather blue colors, but are certainly evolved, and thus including them in the plots could have raised confusion. Virtually all these evolved giants should have passed the second mixing episode. Table 3 indicates that whereas most of these stars have indeed a very low lithium content, a few of them have $\log n(\text{Li})$ still larger than 1. Among these, three are known binaries (HD 469, HD 39937, and HD 85655). There is again an indication that binaries may have higher lithium than single stars and this could be due, in turn, to reduced extra-mixing in the giant phase. Actually, if all the Li-rich evolved giants in our sample turned out to be binaries, with “anomalous” rotation and rotational history with respect to single stars, this would provide an additional indication that the extra mixing process is linked to rotation (e.g., Charbonnel et al. 1998).

6. Summary and conclusions

We have addressed the problem of post-main sequence lithium evolution using new lithium data for a large sample of Pop. I subgiant stars, complemented by data from the literature. The availability of Hipparcos parallaxes has allowed us to infer absolute magnitudes for our sample stars and for the stars in the samples from the literature. We were thus able to locate the stars on the C-M diagram, to constrain their evolutionary status, and to derive masses and ages.

Our analysis indicates that, as it is the case for MS stars and giant stars, subgiants are characterized by a large spread in $\log n(\text{Li})$ and that there is not a one-to-one lithium-mass or lithium-age correlation. In particular, among \sim solar-mass stars in the same evolutionary status as β Hyi, stars are observed with

a high lithium content ($\log n(\text{Li}) > 2$), but also a large fraction of stars that do not show detectable lithium. As well known, the same is observed among old MS stars in the field and in the open cluster M67, where stars as depleted in lithium as the Sun are present together with stars that have at least a factor of ten higher lithium. This, and in particular the fact that β Hyi-like stars are not systematically more lithium rich than solar-like stars, suggests that lithium-rich evolved stars like β Hyi are simply the evolved counterparts of stars that have depleted a small amount of lithium during MS lifetime, rather than stars like the Sun that end their MS lifetime as lithium poor stars and then dredge-up lithium which was diffused downward and stored below the convective zone.

Our analysis confirms that first dredge-up dilution is completed around $B-V = 0.7$ or $T_{\text{eff}} = 5600\text{--}5700$ K, independently on mass and metallicity. Several stars which have undergone dilution, but have not yet reached the position where RGB extra-mixing is thought to occur, show significantly lower lithium than the predicted values by first dredge-up computations. Since not only solar-type stars, but also more massive stars (and, in particular stars in the lithium dip) may leave the MS depleted in lithium, it is not surprising that a fraction of subgiants show a lower lithium than models predictions, which assume that stars leave the MS with their initial lithium content. Our analysis shows that this is indeed the case and that the fraction of lithium rich (or lithium poor) stars among post-dredge up stars in our sample is consistent with what expected based on the observed distribution of Li abundances among stars that have just left the MS.

The signature of the second mixing episode, which occurs when the hydrogen burning shell reaches the chemical discontinuity created by the convective envelope at its maximum extent, is evident in the $\log n(\text{Li})$ vs. M_{bol} distribution of our sample stars. The luminosity of this evolutionary phase, however, seems to be lower than predicted by Charbonnel (1994), at variance with the results of Carretta et al. (1998) for Pop. II stars, but in closer agreement with the predictions of Bertelli et al. (1998) models. Additional lithium observations would help putting more quantitative constraints on the luminosity where extra-mixing becomes efficient and would provide feedback to the models; in addition, CNO observations of our sample stars and, in particular, $^{12}\text{C}/^{13}\text{C}$ ratios would be extremely useful in this respect.

Finally, among clump giants or stars more evolved than the RGB bump, stars are observed with $\log n(\text{Li})$ close to the theoretical predictions of the first dredge-up, i.e., stars that do not seem to have undergone significant extra-mixing. Some (but not all) of them are binaries or active stars, suggesting that the extra-mixing mechanism may be linked to rotation. $^{12}\text{C}/^{13}\text{C}$ ratios would indeed be useful also for these stars.

Acknowledgements. We are indebted to P. Bouchet and R. Vega for carrying out near-IR observations and for reducing the data. We thank J.R. de Medeiros for providing us rotational velocities. Extensive use was made of the SIMBAD database maintained by the Centre de Donnée astronomiques de Strasbourg.

References

- Anthony-Twarog B.J., Laird D., Payne D., Twarog B.A., 1991, AJ 101, 1902
- Balachandran S., 1990, ApJ 354, 310
- Balachandran S., 1995, ApJ 446, 203
- Barrado y Navascués D., Fernández-Figueroa M.J., García López R.J., De Castro E., Cornide M., 1997, A&A 326, 780
- Barrado y Navascués D., De Castro E., Fernández-Figueroa M.J., Cornide M., García López R.J., 1998, A&A 337, 739
- Bertelli G., 1998, private communication
- Bertelli G., Bressan A., Chiosi C., et al., 1994, A&AS 106, 275
- Boesgaard A.M., Tripicco M.J., 1986, ApJ 302, L49
- Bouchet P., 1989, ESO Operating Manual #11
- Bouchet P., Schimder F.X., Manfroid J., 1991, A&AS 91, 490
- Brown J.A., Sneden C., Lambert D.L., Dutchover E., 1989, ApJS 71, 293
- Carretta E., Gratton R.G., 1997, A&AS 121, 95
- Carretta E., Gratton R., Sneden C., Bragaglia A., 1998, In: the Proceedings of Galaxy Evolution: Connecting the Distant Universe with the Fossile Record. In press
- Cayrel de Strobel, Soubiran C., Friel E.D., Ralite N., Francois P., 1997, A&AS 124, 299
- Chaboyer B., Demarque P., Pinsonneault M.H., 1995, ApJ 441, 876
- Charbonnel C., 1994, A&A 282, 811
- Charbonnel C., 1995, ApJ 453, L41
- Charbonnel C., Brown J.A., Wallerstein G., 1998, A&A 332, 204
- Clementini G., Carretta E., Gratton R.G., Sneden C., 1999, MNRAS, in press
- De Medeiros R., Do Nascimento J.D Jr., Mayor M., 1997, A&A 317, 701
- Dravins D., Lindgren L., Nordlund A., Vandenberg D.A., 1993, ApJ 403, 385
- Dravins D., Lindgren L., Vandenberg D.A., 1998, A&A 330, 1077
- Duncan D.K., 1981, ApJ 248, 651
- Duncan D.K., 1984, ApJ 278, 806
- Favata F., Barbera, M., Micela G., Sciortino S., 1995, A&A 295, 147
- Favata F., Micela G., Sciortino S., 1997, A&A 322, 131
- Fekel F.J., Balachandran S.C., 1993, ApJ 403, 708
- Fernández-Figueroa M.J., Barrado D., De Castro E., Cornide M., 1993, A&A 264, 373
- García López R.J., Rebolo R., Beckman J.E., 1988, PASP 100, 1489
- Gilroy K.K., 1989, ApJ 347, 835
- Gratton R.G., Sneden C., 1990, A&A 234, 366
- Gratton R.G., Sneden C., 1991, A&A 241, 501
- Gratton R.G., Sneden C., 1994, A&A 287, 927
- Gratton R.G., Carretta E., Castelli F., 1996, A&A 314, 191
- Hauck B., Mermilliod M., 1980, A&AS 40, 1
- Hearnshaw J.B., 1972, MNRAS 77, 55
- Hoffleit D., Jascheck C., 1982, The Bright Star Catalogue. Yale Observatory, New Haven
- Iben I., 1965, ApJ 142, 1447
- Iben I., 1967a, ApJ 147, 624
- Iben I., 1967b, ApJ 147, 650
- Kaper L., Pasquini L., 1996, ESO Operating Manual, 3p6CAT-MAN-0633-0001
- Kurucz R.L., Furenlid I., Brault J., Testerman L., 1984, Solar Flux Atlas from 296 to 1300 nm, National Solar Obs., Atlas No. 1
- Kurucz R.L., 1993, CD-ROM 13 and CD-ROM 18
- Kurucz R.L., 1995, private communication
- Olsen E.H., 1983, A&AS 54, 55
- Olsen E.H., 1993, A&AS 102, 89

- Pallavicini R., Randich S., 1994 In: Crane P. (ed.) Proceedings of the ESO/EIPC Workshop on Light Element Abundance. p. 311
- Pallavicini R., Cerruti-Sola M., Duncan D.K., 1987, A&A 174, 116
- Pasquini L., Liu Q., Pallavicini R., 1994, A&A 287, 191
- Pasquini L., Randich S., Pallavicini R., 1997, A&A 325, 535
- Pilachowski C.A., Sneden C., Booth. J., 1993, ApJ 407, 699
- Pinsonneault M.H., 1997, ARA&A 35, 557
- Randich S., Gratton R., Pallavicini R., 1993, A&A 273, 194
- Randich S., Giampapa M.S., Pallavicini R., 1994, A&A 283, 893
- Schuster W.J., Nissen P.E., 1988, A&AS 73, 225
- Schuster W.J., Nissen P.E., 1989, A&A 221, 65
- Soderblom D.R., Pilachowski C.A., Fedele S.B., Jones B., 1993, AJ 105, 2299
- Spite F., Spite M., Peterson R.C., Chaffee F.H., 1987, A&A 172, L8
- Swenson F.J., Faulkner J., Iglesias C.A., Rogers F.J., Alexander D.R., 1994a, ApJ 422, L79
- Swenson F.J., Faulkner J., Rogers F.J., Iglesias C.A., 1994b, ApJ 425, 286

Note added in proof: soon after the present paper was accepted for publication, a paper on a similar topic was published (Lèbre et al. 1999, A&A 345, 936). It seems that their and our results are generally consistent, but a detailed comparison could not be carried out since we became aware of that paper only at the proofs stage.